5844 *Macromolecules* **1993,** *26,* 5844–5851

Determination of Interdiffusion in Thin Polymer Films Using FTIR Reflection Absorption Spectroscopy

H. Eklind and T. Hjertberg*

Department of Polymer Technology, Chalmers University of Technology, S-41296 Göteborg, Sweden

Received February 10, 1993; Revised Manuscript Received August 3, 1993[®]

ABSTRACT: FTIR reflection absorption spectroscopy (RAS) has been used to develop a method to study interactions in artificial interphases of polymer blends. Two films of poly(vinyl ethyl ether) (PVEE) and poly(ethylene-*co*-acrylic acid) (EAA), with thicknesses ranging from 100 to 600 Å each, were solution cast on a gold surface and annealed at 125 °C for different times. The carboxylic acid groups of EAA differently hydrogen bonded to different species, and the diffusion of EAA and PVEE into each other could be followed by studying the C=O bands in the infrared spectra. One advantage of studying these thin films instead of entire blends is that the influence of the bulk properties is reduced, and we therefore observe the behavior of the molecules in the artificial interphase itself. Quantitative measurements of the amount of hydrogen bonds made it possible to calculate the diffusion constant and also to obtain a measure of the interphase thickness after different annealing times.

Introduction

Blending of polymers is an attractive method to obtain new polymeric materials. The ultimate goal is to achieve an optimal material by combining favorable properties from the starting materials. As most polymer pairs are incompatible, the properties of the complex material will be strongly influenced by interactions between the phases. In many cases the addition of "compatibilizers", e.g., block or graft copolymers, may increase the interactions and enlarge the interdiffusion layer, or "interphase", between the phases. The interphase is considered as a third phase in the immiscible polymer blend and has its own characteristic properties.[1] Formation of a more diffuse layer between the phases by a compatibilizer, giving less distinct phase boundaries, thus leads to improved mechanical properties of the blend. Although the importance of the interphase is recognized, there is a lack of detailed knowledge about interactions in interphases in polymer blends.

One reason for this is the fact that it is very difficult to observe the small volume fraction occupied by the interphase in a polymer blend. In studies of polymer diffusion it is generally self-diffusion coefficients that have been determined,[2–4] and only in some cases mutual diffusion, or interdiffusion, has been studied. The most frequently used methods of studying diffusion processes are different scattering, spectroscopic, fluorescence, and radioactive techniques.[2,3] It should be noted that in most of these methods, the studied thickness of the interdiffusion layer has been on the order of micrometers. This is much thicker than the expected thickness of the interphase in incompatible polymer blends, where the domain size of the dispersed phase typically is in the range of microns or fractions of a micron. Shilov et al.[5] suggested an interphase thickness of 0.5–4.0 nm for a particular immiscible binary system, but the thickness is thought to be even thinner for other systems. In a partially miscible blend, the thickness of the interphase depends on the miscibility between the polymers but is still much thinner than the size of the dispersed phase. A rule of thumb is that the better the miscibility of a system, the thicker is the interphase.

The aim of this work was to develop a method to study the formation of thin interphases, 50–500 Å, between two polymers in a system with some extent of miscibility. For this, we chose the Fourier-transform infrared reflection absorption spectroscopy (FTIR-RAS) technique. If two polymers have functional groups that interact with each other, the absorbance bands in their infrared spectra may shift, and studying these shifts has proved to be an excellent and straightforward method of studying interactions in polymers, especially when hydrogen bonding is involved. Interactions involving hydrogen bonding occur in many different species, as, for example, between carboxylic acid, urethane, and amide groups, and it is a very important factor in the formation of crystal structures. Characterization of the hydrogen bond in polymers has been done with two different methods, i.e., thermodynamic and spectroscopic measurements. Presently, spectroscopy (IR, Raman, fluorescence, NMR, etc.) is most powerful.[6] We have chosen to study the hydrogen bond between an acrylic acid and an ether. Polymer films of poly(ethylene-*co*-acrylic acid) (EAA) and poly(vinyl ethyl ether) (PVEE), with thicknesses ranging from 100 to 600 Å, have been investigated. In the present work, quantifying the fraction of "free" and hydrogen-bonded groups was most important, and of the spectroscopic methods, infrared spectroscopy is by far most applicable for obtaining this information. More details about different infrared techniques have been discussed by a number of others.[7,8]

Other infrared techniques have also been used to study interdiffusion in polymers. Van Alsten and Lustig[9] used attenuated total reflectance (ATR) to study diffusion of a thin film (0.02–0.5 μm) of one polymer into a relatively thick film (25–125 μm) of a second polymer. This technique seems to be useful to determine mutual diffusion constants but implies that thicker regions than the interphase are studied. High et al.[10] used transmission FTIR to study interdiffusion in polymer films of poly(ethylene-*co*-methacrylic acid) (EMAA) and poly(vinyl methyl ether) (PVME). The benefit of RAS compared to ATR and ordinary transmission FTIR is that it makes it possible to look at thinner films and thus to focus more specifically on the interphase, especially if the system has limited miscibility. A method to study interphases in polymer blends with nuclear magnetic resonance spectroscopy (NMR) has been developed by Afeworki et al.[11–14] They show that their results only originate from the

---

* To whom correspondence should be addressed.

[®] Abstract published in *Advance ACS Abstracts,* October 1, 1993.

0024-9297/93/2226-5844$04.00/0

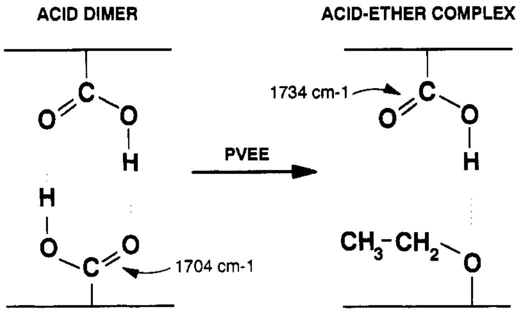

Figure 1. Schematic diagram of a self-associated carboxylic acid dimer together with the formation of a carboxylic acid–ether complex.

interphase, but the experiments are difficult to perform and very time-consuming. Compared to NMR, the RAS technique requires only common commercial infrared equipment and takes much less time. The RAS technique was first developed by Francis and Ellison[15] and Greenler[16] and has become a widely used method in studying absorbed species on metal surfaces, but it has not yet become a frequently used method for studying interactions in polymer blends. We have previously used the method to study adhesion of polymers on alumina surfaces.[17,18] In this study we have used the metal surface only as a reflector of the infrared beam and as a support for the polymer films. Using the RAS technique, we were able to follow the gradual growth of the interphase through annealing, with no interference of the bulk, by studying the interactions between the two polymers. The thickness of the interphase was in the range 100–600 Å, which is much smaller than earlier reported results obtained with infrared techniques. It should also be stressed that we have not used specifically marked polymers.

Theoretical Consideration

Thermodynamic Equilibria. The thermodynamics of polymer blends has been studied by a number of researchers during the past decades, and a good review has been made by Utracki.[1] To describe the hydrogen bond, one can use certain association models, which have been summarized by Acree[19] and Coleman.[6] As in other types of equilibrium equations, there are competing equilibria; i.e., a number of hydrogen bonds can be formed between the different molecular groups involved. In a polymer containing carboxylic acid groups, the acid groups exist as "free" groups (nonassociated) or can form dimers (self-associated) through mutual hydrogen bonding between one hydroxyl group and one carbonyl group. If we add an ether, which does not self-associate, some of the acid hydroxyl groups will form hydrogen bonds to the ether oxygens instead,[6] which is shown in Figure 1. This leads to a release of some carbonyl groups, which no longer will be hydrogen bonded. The amount of these carbonyl groups is the same as the number of acid–ether hydrogen bonds formed, and we call them "free" C=O groups. We let B be the nonassociated carboxylic acid groups in EAA and A be the nonassociated ether groups in PVEE. The equilibria could thus be written as

$$\mathrm{B} + \mathrm{B} \overset{K_B}{\rightleftarrows} \mathrm{BB} \tag{1}$$

$$\mathrm{A} + \mathrm{B} \overset{K_A}{\rightleftarrows} \mathrm{AB} \tag{2}$$

Here, BB and AB mean the self-associated acid dimer and the hydrogen-bonded acid–ether complex, respectively. The equilibrium constants K_A and K_B are defined by Flory[20] in terms of volume fractions, which in our case gives us the constants as[21,22]

$$K_B = \frac{\Phi_{BB}}{{\Phi_B}^2}\frac{1}{2} \tag{3}$$

$$K_A = \frac{\Phi_{AB}}{\Phi_A\Phi_B}\left(\frac{r}{r+1}\right) \tag{4}$$

where Φ_{BB}, Φ_B, Φ_{AB}, and Φ_A are the volume fractions of the corresponding structures. The factor r is the ratio of the molar volumes of the average polymer repeating units, i.e., V_A/V_B. We assume that the volume fraction of two interacting groups is the same as the sum of the two individual groups. In accordance with Coleman et al.,[23] the stoichiometry of the system can thus be derived from eqs 3 and 4. In determining the equilibrium constants, we used infrared data from pure EAA (K_B) and a EAA–PVEE mixture (K_A). In pure acid copolymer (superscript 0) the volume balance (assuming that we do not have any anhydride or ester groups present) then becomes

$${\Phi_B}^0 + {\Phi_{BB}}^0 = 1 \tag{5}$$

The fraction of free C=O groups in the pure copolymer, ${f_F}^0$, i.e., the fraction of non-hydrogen-bonded acid groups, is defined as

$${f_F}^0 = \frac{{\Phi_B}^0}{{\Phi_B}^0 + {\Phi_{BB}}^0} = {\Phi_B}^0 \tag{6}$$

Together with eq 3, this gives K_B as

$$K_B = \frac{1 - {f_F}^0}{2({f_F}^0)^2} \tag{7}$$

If FTIR data from a mixture of EAA and PVEE are known, the constant K_A can also be determined from eqs 3 and 4.

Fraction of Free C=O Groups. When we let two polymers diffuse into each other, the concentration changes in a specific volume element with time, t. A way of expressing the diffusion process at a specific time in a carboxylic acid–ether system in terms of volume fractions and equilibrium constants has been presented by High et al.[10] The contribution to the absorption in the infrared region at a specific wavelength, dA, in a thin slice of material with a thickness of dz in the diffusion direction is proportional to the absorptivity, a, the concentration of the species, and the path length. The total absorbances of the hydrogen-bonded C=O groups in the dimerized carboxylic acid groups (index D) and for the free C=O groups of each EAA in the acid–ether complexes (index F) could thus be expressed as

$$A_D(t) = C\int_{-L_B}^{L_A} a_D\, \Phi_D(z,t)\, dz \tag{8}$$

$$A_F(t) = C\int_{-L_B}^{L_A} a_F\, \Phi_F(z,t)\, dz \tag{9}$$

L_A and L_B are the thicknesses of the PVEE and EAA films, respectively. Φ_D and Φ_F are the volume fractions of the acid dimer (Φ_{BB}) and the acid–ether complex (Φ_{AB}), respectively, as described previously. C is a proportionality constant originating from the fact that the beam path length is not equal to the thickness of the sample in the RAS technique, in contrast to transmission FTIR. C can vary if the orientation is different in the samples, but we assume that C has a constant value for each sample thickness. $A_D(t)$ and $A_F(t)$ can then be used to calculate the fraction of free C=O groups, f_F, after the diffusion time, t, as

$$f_F(t) = \frac{A_F(t)}{A_F(t) + \frac{1}{\text{ar}} A_D(t)} \tag{10}$$

where the parameter "ar" is the ratio of the absorptivities, a_D/a_F.

Diffusion Process. In all derivations it is assumed that the thermodynamic equilibria (eqs 1 and 2) are reached almost instantly, i.e., that the diffusion process is much slower than the kinetics of these equations. To calculate $f_F(t)$ we must know $\Phi_D(z,t)$ and $\Phi_F(z,t)$ as a function of distance, z, and time, according to eqs 8–10. These can be calculated if it is possible to determine the total volume fraction of EAA, $\Phi_{B,tot}(z,t)$, for specific values of z and t. Fick's second law can be expressed as a differential equation as in eq 11, assuming complete miscibility in the system, with the presumptions that the mutual diffusion constant, D_{AB}, is independent of composition (usually not exactly true) and that the partial specific volume of EAA is constant.[10,24]

$$\frac{\partial \Phi_{B,tot}(z,t)}{\partial t} - D_{AB} \frac{\partial^2 \Phi_{B,tot}(z,t)}{\partial z^2} = 0 \tag{11}$$

This second-order partial differential equation could then be solved with the initial (eqs 12 and 13) and open-boundary (eqs 14 and 15) conditions shown below.

$$t = 0; \quad z < 0; \quad \Phi_{B,tot} = 1 \tag{12}$$

$$t = 0; \quad z > 0; \quad \Phi_{B,tot} = 0 \tag{13}$$

$$t > 0; \quad z = -\infty; \quad \Phi_{B,tot} = 1 \tag{14}$$

$$t > 0; \quad z = +\infty; \quad \Phi_{B,tot} = 0 \tag{15}$$

The validity of these conditions will be discussed later. Equations 11–15 are satisfied by the standard error function solution:

$$\Phi_{B,tot}(z,t) = \frac{1}{2}\left(1 - \operatorname{erf}\left(\frac{z}{2\,(D_{AB}\,t)^{1/2}}\right)\right) \tag{16}$$

With these conditions, data from FTIR experiments could be used to determine a value of D_{AB}, and this could further be used to obtain an estimation of the interphase thickness after different treatment of the system.

Experimental Section

Materials. Both polymers employed were obtained from Scientific Polymer Products, Inc. The random EAA copolymer contains 20 wt % acrylic acid (EAA[20]), which corresponds to 8.8 mol % acrylic acid groups. DSC analysis showed that EAA[20] has a broad melting interval (from +25 to +110 °C). The glass transition temperature could not be detected with DSC but is probably located well below room temperature. The molecular weight has been determined previously by SEC analysis ($\bar{M}_w$ = 17200, $\bar{M}_n$ = 1700) by Flodin et al.,[25] and the reported density was 0.960 g/cm^3. PVEE has a molecular weight of 118000, a glass transition temperature at −30 °C, and a density of 0.95 g/cm^3, according to the manufacturer. Both polymers were used as received without further purification.

Sample Preparation. Gold plates were made by first sputtering a glass plate with a 10-nm layer of a chromium–nickel alloy to obtain a better attachment of the gold layer and then sputtering the plate with a 200-nm layer of gold. Gold was used as the outer metal surface due to its high reflectivity and its negligible interactions with other materials. The polymer films were then cast through vaporization of polymer solutions with concentrations of 10–50 mg of polymer per 100 mL of solvent. To get the desired film thickness, the necessary solution volume per unit area was first calculated. Four different thicknesses were used for each film layer: 100, 250, 400, and 600 Å. Thicker films were not used due to the fact that absorption in the carbonyl region is linear only for a thickness approximately up to 2000 Å with the RAS technique according to Yoshida and Ishida;[26] i.e., the beam does not properly penetrate thicker films. The films of EAA[20] and PVEE were of equal thickness in all samples. EAA[20] was dissolved in a mixture of decalin and 1-butanol (3:1 by volume). The solution was heated to 80 °C for at least 30 min, and then the appropriate volume was cast onto the gold plate. EAA[20] was cast first because it is more difficult to dissolve. To minimize inevitable mixing of EAA[20], PVEE was dissolved in *n*-hexane at room temperature and cast on the dried EAA[20] film in a similar way. After each polymer layer was cast, the plate was carefully flushed with nitrogen gas at room temperature to remove as much solvent as possible. The polymer-covered gold plates were then annealed in air at 125 °C, which is above the glass transition and melt temperatures of the polymers, for various times up to more than 24 h and then cooled to room temperature.

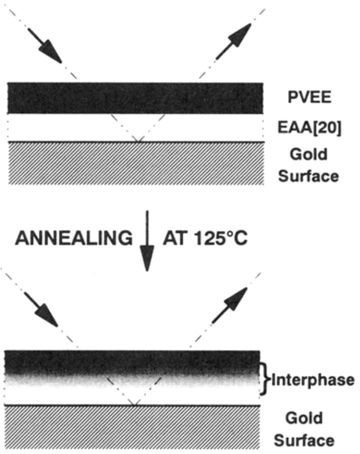

Figure 2. Schematic representation of the setup for the RAS experiments.

Instrumentation. FTIR measurements were performed with a Perkin-Elmer System 2000 FT-IR. A schematic drawing of the experimental setup is shown in Figure 2. When doing the measurements on the polymer-covered gold plates, we used a reflection absorption spectroscopy (RAS) accessory with a liquid-nitrogen-cooled mercury–cadmium telluride (MCT) detector. The angle of incidence was fixed at 80°. The sample chamber was carefully purged with dry air for 40–60 min before scanning to remove water, which has a high absorption in the carbonyl region. As a reference, the water absorption peak at 1654 cm^{-1} was used, and the purging was continued until this peak no longer was seen before final scanning was started. All gold plate samples were scanned 100 times, and the resolution was 4 cm^{-1} (higher resolution gave too much noise). All spectra were curve fitted to determine the carbonyl absorption (which is proportional to the area under the curve in the absorption spectra) of the different species in each sample. This made it possible to calculate the experimental value of the fraction of free C=O groups in EAA[20]. To determine the diffusion constant and the extension of the interphase, the diffusion process was simulated with a computer. It was taken into consideration that the absorption of the free C=O groups was overlapped by ester C=O groups in the infrared spectra.

Thermal properties were measured with DSC and TGA instruments (Perkin-Elmer Thermal System 7). TGA measurements were performed at a constant temperature (125 °C) for 8 h in a nitrogen environment. We also used a Varian VXR-300 S NMR instrument to characterize EAA[20]. Both ^{1}H and ^{13}C NMR spectra were taken. To study the surface topography of the samples, we used a JEOL JSM-820 L scanning electron microscope (SEM), and the acceleration voltage was then 5 kV.

Determination of Constants. The ratio of the absorptivities of the free and hydrogen-bonded C=O groups, ar, was calculated through comparing spectra of the same sample kept at 125 °C for different times. The value of ar could then be calculated as in eq 17.

$$\mathrm{ar} = \frac{a_D}{a_F} = \frac{A_D(\text{time } 1) - A_d(\text{time } 2)}{A_F(\text{time } 2) - A_F(\text{time } 1)} \qquad (17)$$

To calculate the course of the diffusion process, the equilibrium constants, K_A and K_B, had to be determined. This was done with transmission spectroscopy using a triglycine sulfate (TGS) detector at room temperature, and the samples were scanned 50 times with a resolution of 4 cm^{-1}. K_B was determined from infrared data of EAA[20], which was first dissolved in a mixture of decalin and 1-butanol (3:1 by volume), then cast on a KBr disk, and finally annealed at 125 °C for 200 min. Curve fitting made it possible to separate the absorptions of free acid monomer, ester, and self-associated acid dimer groups. The previously described absorptivity ratio between the C=O groups in the dimer and the free C=O groups, ar, was also assumed to be valid for the acid dimer–ester C=O absorptivity ratio. Calculations from the experimental results gave a value of K_B. Another solution was made of equal parts per volume of EAA[20] and PVEE in decalin, 1-butanol, and n-hexane (3:1:4 by volume), and the mixture was cast on a KBr disk. The polymer film was annealed at 125 °C for 15 h to reach as close to the thermodynamic equilibrium of the blend as possible. The transmission spectra taken at room temperature, together with the value of K_B, was used for determination of K_A. The annealing process and the cooling of these films were performed in a similar way as with the gold plate samples.

Diffusion Calculations. Diffusion constants were calculated for each experimental value of f_F, i.e., for each value of film thickness ($L = L_A = L_B$) and annealing time. The overall diffusion constant for an applied film thickness, $D_{AB}(L)$, was taken as the logarithmic mean value of $D_{AB}(L,t)$ for different diffusion times.

Results and Discussion

FTIR- and TGA-Data. FTIR spectra for the samples with predicted film thicknesses of 100 and 250 Å are shown in Figure 3. Originally, the peak heights were relatively smaller for the samples with longer annealing times, due to different absorptivities, but the spectra have been scaled so as to be more clear. In the spectra of EAA[20] alone (no PVEE cast on top of it), denoted "–" in the figures, the smaller peak at ca. 1740 cm^{-1} corresponds mostly to the C=O group of an ester impurity (discussed later), while the larger peak at 1704 cm^{-1} corresponds to the C=O groups of the self-associated dimer.[27] We see that the amount of the acid dimer decreases, while the acid–ether hydrogen bond increases in amount,[28] represented by the free C=O absorption at 1734 cm^{-1}, with longer annealing times at 125 °C. This process proceeds gradually and is easy to follow. A comparison of parts a and b of Figure 3 shows that the diffusion process takes longer for the thicker films, due to longer diffusion paths. The spectra for the samples with 400- and 600-Å-thick films are similar, besides that the transitions from the acid dimer to the acid–ether complex take even longer times.

Even though the C=O absorptions of the thin films are very small (ranging from <0.001 absorption units), repeated experiments show that the results were very reproducible. Casting very thin films from a solution, as done in this work, is not the best way of getting uniform films, but it is a simple method to obtain films of desired thicknesses. Although there were small variations between spectra of different samples with the same thickness and temperature treatment, it was easy to follow the diffusion process in the spectra from one time to another. The thermal stability was also examined for the two polymers using a TGA instrument. Neither EAA[20] nor PVEE lost any weight (except for some solvent in PVEE) when the samples were kept at 125 °C for 8 h in a nitrogen environment. This shows that the two polymers are not easily degraded at the experimental conditions.

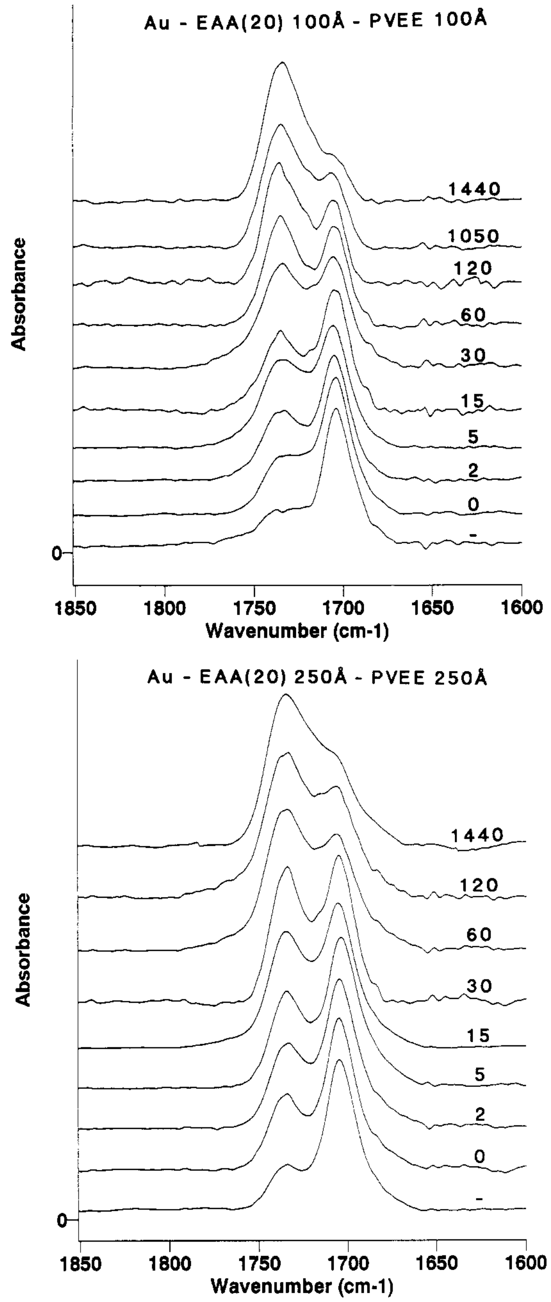

Figure 3. FTIR spectra in the carbonyl region of the EAA[20]–PVEE interdiffusion couple recorded as a function of annealing time (minutes) at 125 °C. The film thicknesses are in (a, top) 100 Å and (b, bottom) 250 Å.

The Absorptivity Ratio. To calculate the fraction of free C=O groups, the absorptivity ratio, ar = a_D/a_F, was calculated for many samples with different film thicknesses. The overall average value was determined to be 2.2 and was considered to be independent of the film thickness. This value could be compared to the value for the EMAA–PVME system mentioned previously, which was determined by Lee et al.[28] to be ca. 1.6. The higher value could be due to the fact that we have used a different technique to determine ar; i.e., we applied the RAS technique and annealed each sample at a constant temperature for different times, while Lee et al. used transmission spectroscopy and annealed at different temperatures. The difference could also be due to the fact that we have used a slightly different chemical system, have other experimental conditions, or have larger un-

Table I. Data for Determination of K_A and K_B

	measd C=O absorbance area (%)			
constants	1748 cm^{-1}	1734 cm^{-1}	1704 cm^{-1}	calcd value^a
K_B	1		99	1×10^3
K_A	0.3^b	71.4	28.3	30

^{a} ar = 2.2. ^{b} Calculated using the value of K_B.

certainties in the curve fitting of the FTIR spectra for our thin films.

K_A and K_B. The two thermodynamic equilibrium constants, K_A and K_B, had to be determined to calculate the fraction of free C=O groups during the diffusion process. Data for the determination of the constants are shown in Table I. In a fast survey of a transmission spectrum of EAA[20], it looks like there are only two peaks in the carbonyl region, one smaller at ca. 1740 cm^{-1} and one larger at 1704 cm^{-1}. The peak at 1704 cm^{-1}, representing the acid dimer, is well defined and usually dominating in carboxylic acid species.[27] Carboxylic acid anhydrides have two stretching bands in the carbonyl region, but a second peak between 1820 and 1770 cm^{-1}, which exists in carboxylic acid anhydrides, cannot be seen for EAA[20]. The peak at 1740 cm^{-1} is then likely to come from an ester impurity or a free acid. Studying the peaks in other regions gives no certain support in either direction. When doing a curve fitting, we also observed a smaller peak at 1748 cm^{-1}, besides a larger peak at 1740 cm^{-1}. According to Bellamy,[29] the frequency difference between the free acid and the acid dimer is always close to 45 cm^{-1}, while the normal ester C=O stretch is found at ca. 1740 cm^{-1}. The presence of an ester group was also directly indicated in a ^{13}C NMR spectrum of EAA[20], where we could see two different carbonyl carbons. The interpretation of the spectrum points to a methyl ester. We then make the conclusion that the peak at 1748 cm^{-1} is free acid (44-cm^{-1} difference) and the peak at 1740 cm^{-1} is an ester impurity. Ester impurities in similar copolymers have also been found by others[10,27,30] and were probably incorporated during polymerization. Using the equations described previously, we then calculated the value of K_B to be 1×10^3 at the conditions used.

The EAA[20]–PVEE blend sample was prepared by casting one solution of the two polymers on a KBr disk and then letting the solvent evaporate at atmospheric pressure at room temperature. By doing so, it is not sure that the cast blend was at thermodynamic equilibrium, due to different solubility of the two polymers at the ruling conditions. The following annealing had as a purpose to reach as close to equilibrium as possible, i.e., to reach $f_{F,\max}$. If the equilibrium was not reached after subsequent annealing, this would affect the value of K_A. In the spectrum of the EAA[20]–PVEE blend it was easy to distinguish two distinct peaks, one for the self-associated acid dimer at 1704 cm^{-1} and one for the free C=O group of the acid–ether complex at 1734 cm^{-1}, respectively. However, it was not possible to separate with good significance the third expected peak for the nonassociated carboxylic acid group. Therefore, the value of K_B was used in the equations to calculate the volume fractions, giving a K_A value of 30 at our experimental conditions. The difficulty in determining different volume fractions could cause incorrect values of K_A and K_B. These problems could then give incorrect calculated values of the fraction of free C=O groups, but small deviations from the real values will not cause any major errors in the diffusion calculations.

Both K_A and K_B were determined using transmission spectra, while all other spectra were recorded with RAS. Using two different techniques in the experiments could affect the results and is therefore a source of error. The reason this was done was that it was too difficult and uncertain to use the RAS technique for the determination of the constants.

The Diffusion Process. As shown before, the diffusion process is quite easy to follow with this infrared technique. To obtain a measure of the thickness of the interphase that is formed due to the diffusion, we have calculated diffusion constants according to the equations above. This exercise is not made in the attempt to actually determine the absolute diffusion constant but more to give a qualitative picture of the changes due to annealing. The fractions of free C=O groups determined experimentally are given as dots in Figure 4a–d for the systems with 100-, 250-, 400-, and 600-Å film thicknesses of each polymer layer (note the slightly different time scales). The solid lines represent the theoretically calculated values using an average overall diffusion constant for each film thickness. To calculate these averages only the data between 5 and 60 min were used. It is obvious that the experimental points deviate from the calculated values both initially and for longer annealing times. For a film assembly without annealing, there should not be any acid–ether hydrogen bonds, but the opposite is clearly seen in the FTIR spectra (Figure 3a–d) marked "0". Pure EEA[20] is not soluble in the solvent used to deposit PVEE, but *n*-hexane might swell EAA[20], which would enable diffusion of PVEE into EAA during deposition. This would certainly influence the calculation of D_{AB}, and as this problem is difficult to avoid completely, data from the first minutes were not used. The initial penetration is, however, considered not to influence the modeling at longer annealing times.

It can also be noticed that the calculated value of D_{AB} increases 1 order of magnitude when the film thickness is increased from 100 to 600 Å; see Table II. One reason could be that there are inhomogeneities on a scale smaller than the width of the infrared beam. A SEM micrograph of a gold plate sample covered with EAA[20] of a nominal thickness of 600 Å showed that the surface is not completely even but contains "droplets" with diameters in the range 1–20 μm. Scratching the surface demonstrated that the polymer covered the plate. Furthermore, scratches on the gold plate were seen through the droplets, so their thickness must be much smaller than their diameter (penetration depth 0.5–1 μm at 5-kV acceleration voltage[31,32]). Casting PVEE on top of EAA[20] did not change the structure of the surface; see the SEM micrograph of 600-Å PVEE on 600-Å EAA[20] in Figure 5. The scratches in the gold plate can be seen, but it is difficult to discern the PVEE layer, which we believe is more homogeneously deposited than the EAA[20] layer.

With decreasing thickness of the EAA[20] layer, the variation in thickness due to the droplets will be relatively larger, as illustrated in Figure 6. In a droplet, with its larger thickness, the time to reach equilibrium will be longer than for the average thickness due to the longer diffusion path. This effect should of course be most obvious for the thin films, and the conversion from acid dimers to acid–ether complexes did indeed slow down faster when thinner films were used, as shown in Figure 4a–d. The diffusion constant will of course also be influenced, which at least partly explains the effect of thickness on D_{AB}. The diffusion constant determined from the sample with 600-Å films is ca. 5×10^{-16} cm^2/s. Probably the value should be even higher due to the nonuniformity

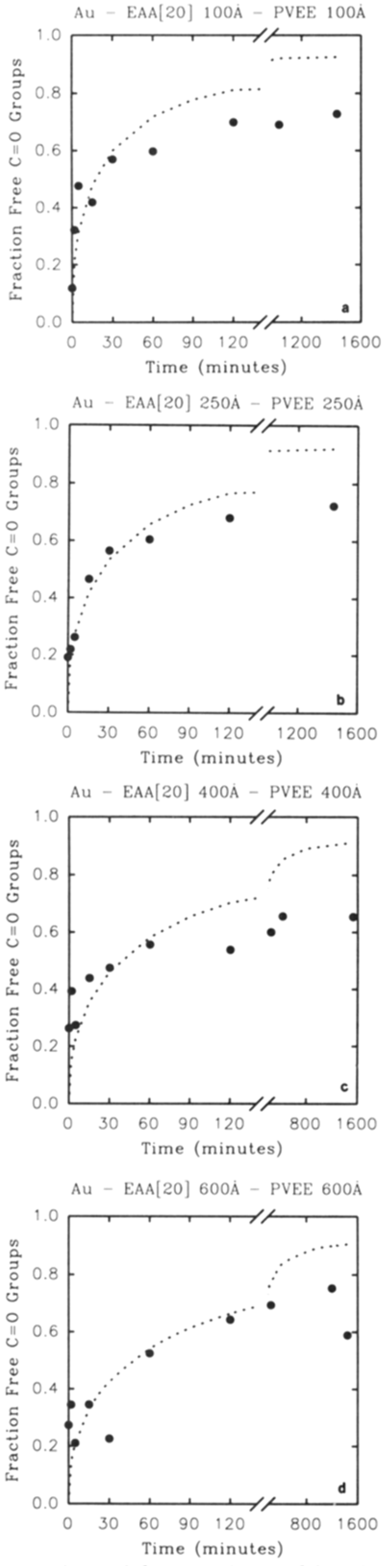

Figure 4. Comparison of the experimental fractions of the free C═O groups (●) to theoretical calculations (dotted lines) as a function of time. The film thicknesses are (a) 100, (b) 250, (c) 400, and (d) 600 Å, and the diffusion constants used in the calculations are presented in Table II.

of the films, but it is still within the expectation range (10^{-16}–10^{-12} cm^2/s) according to Composto et al.[33]

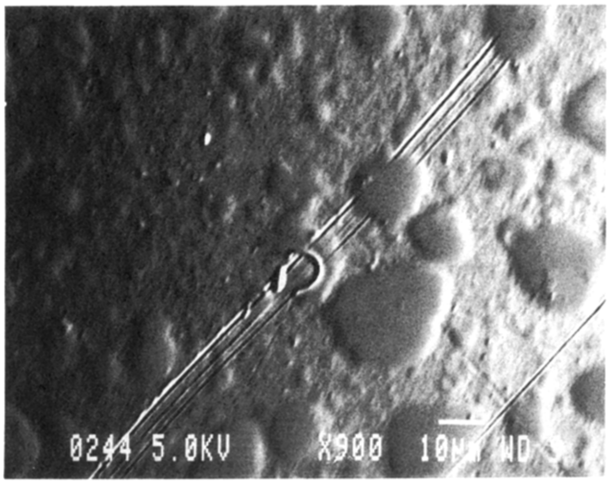

Figure 5. SEM micrographs of a gold surface covered with 600-Å EAA[20] and 600-Å PVEE.

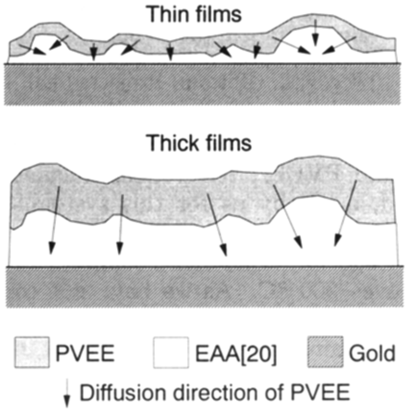

Figure 6. Schematic representation of cross-sections of a gold plate covered with thin and thick polymer films.

Table II. Diffusion Constants for Varying Film Thicknesses

thickness of each film layer, $L_A = L_B$ (Å)	logarithmic mean value of the diffusion constant, D_{AB} (cm^2/s)
100	0.4×10^{-16}
250	2×10^{-16}
400	3×10^{-16}
600	5×10^{-16}

The fit between the experimental and calculated data is best during the first 30–60 min, but for longer times the fraction of free C═O groups is ca. 0.1–0.2 larger than the expected values. Apart from possible effects of the irregular surface, there are some other explanations as well. Mathematically, the deviation at longer annealing times can be described as a decrease in D_{AB}. Physically, this would mean that D_{AB} is dependent on the concentration, which indeed has been reported for other systems.[24]

A more obvious reason for the deviation at longer times is that the model used is based on infinite diffusion paths. This gives a simpler system than assuming closed boundaries. High et al.[10] have shown that both models were in good agreement with the experimental results obtained with EMAA and PVME. They used much thicker films, 0.1–0.5 μm, and consequently longer annealing times. The deviation for the open-boundary model occurred after 10–20 h, compared to 30–120 min in our experiments. It can be concluded that the model based on infinite diffusion paths can be used during the initial stage, i.e., the period which should be of interest for the development of an interphase in a blend.

Finally, another possible source of error is in the assumption of complete miscibility, for which all diffusion equations are derived. If there is a phase separation, due to crystallization or other reasons, the system will form phases of different compositions, which probably will affect the calculated values of f_F. In this work we have done no

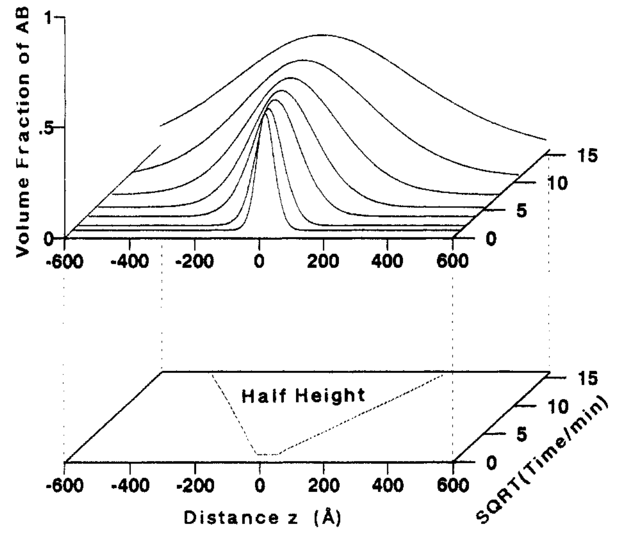

Figure 7. (Top) Volume fraction of the AB complex calculated as a function of distance from the initial surface (where negative and positive values represent the occupation of the initial EAA[20] and PVEE film, respectively) and of the square root of time. $D_{AB} = 5 \times 10^{-16}$ cm^2/s. (Bottom) Projected half-heights.

experiments to measure the extent of miscibility between EAA[20] and PVEE. Theoretical calculations, on the other hand, made by us for this system (the method described by Coleman et al.[23]) indicate that the system is completely miscible in all blend compositions at temperatures above −200 °C. As we have not compared this theoretical calculation with experimental measurements, we cannot say anything about its validity, but we find it reasonable to believe that EAA[20] and PVEE show a high extent of miscibility.

The Interphase. Since we see that the experimental data are in reasonable agreement with the theoretical diffusion calculations (Figure 4a–d), the diffusion theory could be further used to give an estimation of the interphase thickness at various times. Figure 7 shows the calculated volume fraction of associated carboxylic acid–ether complex, Φ_{AB}, at various times for the conditions when the EAA[20] and PVEE films both are 600 Å thick and the diffusion constant has a value of 5×10^{-16} cm^2/s. The maximum calculated value of Φ_{AB} is ca. 0.5. The reason it is not higher is that we have a large stoichiometric excess of ether groups. As a measure of the interphase thickness, we take the full width of the half-heights (fwhh) of these curves. In the lower part of Figure 7 the half-heights are projected and the distance between two lines at a specific time gives fwhh. If we plot fwhh versus time, we see that it is approximately proportional to $t^{1/2}$. A variation of the diffusion constant in the theoretical expressions shows further that fwhh also is proportional to $D^{1/2}$. Linear regression of the calculated fwhh values gives us an approximate expression of the interphase thickness for this EAA[20]–PVEE system as

$$\mathrm{fwhh} = 2 \times 10^{9} D_{AB} t \quad (\text{Å}) \qquad (18)$$

The dependence of the diffusion depth has been shown before[34,35] to be proportional to $D^{1/2}$ and $t^{1/2}$. Using another method to produce very thin, but more homogeneous polymer films, we believe that this infrared technique of studying thin polymer films can be used to determine the interphase thickness and expressed as a function proportional to $D^{1/2}$ and $t^{1/2}$, without any influence of the film thickness.

Conclusions

A method of studying interfacial interactions in polymer blends has been presented in this paper. We succeeded in observing interdiffusion in very thin films (from 100-Å thickness), without influence of the bulk. From FTIR-RAS data the diffusion process could be calculated using a specific model for the hydrogen bonding in the EAA[20]–PVEE system. We obtained values of the overall diffusion constant D_{AB} for the EAA[20]–PVEE system with different film thicknesses using the open-boundary conditions, with the value for the 600-Å films being 5×10^{-16} cm^2/s (the bulk value is probably higher). An approximate value of the interphase thickness has also been established from the diffusion results. Using the volume fraction of the acid–ether complex as a reference, we found the thickness of the interphase, fwhh, to be approximately $2 \times 10^{9} D_{AB} t$ (Å) in the 600-Å films.

We consider that the major advantage of this method is that we can study interactions in films with the same thicknesses as thin interphases, with a minimum of involvement of bulk properties. It seems very likely that this method of investigating interphases could be useful for systems with partial miscibility as well and to obtain a measure of the interphase thickness in these systems. The quantitative judgment is, however, more dependent on the system itself and if there is possible to find appropriate mathematical models which include the interactions in the system. We will do further investigations with polymer systems including a compatibilizer and try to see how the penetration depth of this in the different phases of the constituents of the blend affects the mechanical properties of the polymer bulk.

Acknowledgment. We gratefully acknowledge the National Swedish Board for Industrial and Technical Development (NUTEK) for financial support of this work. We also wish to thank Prof. Dr. Frans Maurer for helpful discussions on the nature of the diffusion process.

References and Notes

(1) Utracki, L. A. *Polymer Alloys and Blends: Thermodynamics and Rheology*; Hanser Publishers: Munich, 1990.

(2) Crank, J.; Park, G. S. *Diffusion in Polymers*; Academic Press Inc.: London, 1968.

(3) Brochard-Wyart, F. *Fundamentals of Adhesion*; Lee, L.-H., Ed.; Plenum Press: New York, 1991.

(4) Vergnaud, J. M. *Liquid Transport Processes in Polymeric Materials: Modeling and Industrial Applications*; Prentice-Hall, Inc.: Englewood Cliffs, NJ, 1991.

(5) Shilov, V. V.; Tsukruk, V. V.; Lipatov, Yu. S. *Vysokomol. Soedin.* **1984**, *A26*, 1347.

(6) Coleman, M. M.; Graf, J. F.; Painter, P. C. *Specific Interactions and the Miscibility of Polymer Blends*; Technomic Publishing Co., Inc.: Lancaster, PA, 1991.

(7) Ishida, H. *Rubber Chem. Technol.* **1987**, *60*, 497.

(8) Culler, S. R.; Ishida, H.; Koenig, J. L. *Annu. Rev. Mater. Sci.* **1983**, *13*, 363.

(9) Van Alsten, J. G.; Lustig, S. R. *Macromolecules* **1992**, *25*, 5069.

(10) High, M. S.; Painter, P. C.; Coleman, M. M. *Macromolecules* **1992**, *25*, 797.

(11) Afeworki, M.; McKay, R. A.; Schaefer, J. *Macromolecules* **1992**, *25*, 4084.

(12) Afeworki, M.; Schaefer, J. *Macromolecules* **1992**, *25*, 4092.

(13) Afeworki, M.; Schaefer, J. *Macromolecules* **1992**, *25*, 4097.

(14) Afeworki, M.; Vega, S.; Schaefer, J. *Macromolecules* **1992**, *25*, 4100.

(15) Francis, A. S.; Ellison, A. H. *J. Opt. Soc. Am.* **1959**, *49*, 130.

(16) Greenler, R. G. *J. Chem. Phys.* **1966**, *44*, 310.

(17) Ulrén, L.; Hjertberg, T. *J. Adhes.* **1990**, *31*, 117.

(18) Strålin, A.; Hjertberg, T. *J. Adhes. Sci. Technol.* **1992**, *6*, 1233.

(19) Acree, W. E. *Thermodynamic Properties of Nonelectrolyte Solutions*; Academic Press: New York, 1984.

(20) Flory, P. J. *Chem. Phys.* **1944**, *12*, 425.
(21) Painter, P. C.; Park, Y.; Coleman, M. M. *Macromolecules* **1988**, *21*, 66.
(22) Painter, P. C.; Park, Y.; Coleman, M. M. *Macromolecules* **1989**, *22*, 570.
(23) Coleman, M. M.; Lee, J. Y.; Serman, C. J.; Wang, Z.; Painter, P. C. *Polymer* **1989**, *30*, 1298.
(24) Crank, J. *The Mathematics of Diffusion*, 2nd ed.; Oxford University Press: London, 1975.
(25) Chihani, T.; Bergmark, P.; Flodin, P. *J. Adhes. Sci. Technol.*, in press.
(26) Yoshida, S.; Ishida, H. *J. Adhes.* **1984**, *16*, 217.
(27) Silverstein, R. M.; Bassler, G. C.; Morrill, T. C. *Spectrometric Identification of Organic Compounds*, 5th ed.; John Wiley & Sons, Inc.: New York, 1991.
(28) Lee, J. Y.; Painter, P. C.; Coleman, M. M. *Macromolecules* **1988**, *21*, 346.
(29) Bellamy, L. J. *The Infrared Spectra of Complex Molecules*, 3rd ed.; Cambridge University Press: Cambridge, 1975; Vol. 1, p 189.
(30) Lichkus, A. M.; Painter, P. C.; Coleman, M. M. *Macromolecules* **1988**, *21*, 2636.
(31) Newbury, D. E.; Joy, D. C.; Echlin, P.; Fiori, C. E.; Goldstein, J. I. *Advanced Scanning Electron Microscopy and X-Ray Microanalysis*; Plenum Press: New York, 1986.
(32) Wells, O. C. *Encyclopedia of Materials Science and Engineering*; Bever, M. B., Ed.; Pergamon Press: Oxford, 1986; Vol. 6, p 4310.
(33) Composto, R. J.; Kramer, E. J.; White, D. M. *Macromolecules* **1988**, *21*, 2580.
(34) Hobbs, S. Y.; Watkins, V. H.; Bendler, J. T. *Polymer* **1990**, *31*, 1663.
(35) Wu, S. *Polymer Interface and Adhesion*; Marcel Dekker: New York, 1982; p 393.